Shear buckling of cylindrical vessels benchmark exercise

M.Dostal & N.Austin
National Nuclear Corporation Limited, Risley, Warrington, UK
A.Combescure
CEA, Centre d'Etudes de Saclay, Gif-sur-Yvette, France
A.Peano & P.Angeloni
ISMES, Bergamo, Italy

1 INTRODUCTION

In Liquid Metal Fast Breeder Reactors (LMFBR) potential shear buckling failures of the primary vessel, induced through seismic excitations, have to be considered. The problem is particularly severe in pool type reactors due to their large size, radius of approximately 10 m, coupled with small wall thicknesses of 50 mm and less. In addition the primary vessel material, typically 316 stainless steel, has a low yield strength at the normal operating temperatures of around 400°C to 500°C. These characteristics tend to make the structure relatively flexible and subject to potential elasto-plastic shear buckling failure.

The buckling analysis of complex structures has always been a difficult problem for the designer due in part to large discrepancies between buckling loads predicted theoretically/analytically and those experimentally observed. The differences are generally caused by a number of factors such as unrealistic boundary conditions, unreliable material data, or imperfection sensitivity.

There are currently many finite element codes available which have the capability to solve buckling problems. However due to the different algorithms and solution techniques employed in each code it cannot be assumed that each is applicable for the analysis of all strucutres. Thus it follows that stringent code validation and verification are necessary exercises to be undertaken before any critical analyses is performed. Verification is defined as the demonstration that the computer code correctly solves the mathematical model irrespectively of the physical validity of the model. On the other hand validation is concerned with an application of computer codes for solving practical problems.

The object of this paper is to provide a comparison of three different computer codes capable of performing buckling analyses and to demonstrate on practical problems the level of accuracy that may be expected in design analyses. Three computer codes were examined ABAQUS, CASTEM (INCA/BILBO) and NOVNL and the computer results were compared directly with experimental data and other commonly used empirical formula. The joint effort was co-ordinated through the CEC Working Group on Codes and Standards AG2.

2 EXPERIMENTAL MODELS

Two thin walled stainless steel models have been investigated in this benchmark study. The cylindrical shell was manufactured by welding a thin stainless steel sheet along an axial seam. The dimesions of the first cylinder (designated cylinder A) were 0.506 m internal diameter 0.263 m high and 0.914×10^{-3} m wall thickness. The second cylinder (designated cylinder B) was 0.201 m internal diameter, 0.1 m high and 1.2×10^{-3} m wall thickness. Relatively massive flanges were brazed onto the shell at both ends to provide fixed boundary conditions. After brazing the circularity of cylinder A was measured at three axial locations where a maximum geometric imperfection of 0.4 mm was found. The lower flange was bolted securely to a rigid base plate while the upper flange was subjected to a horizontal shear load applied by a hydraulic ram or a screw press. This load was increased until buckling of the cylindrical shell was observed and the limit load reached.

The material properties of the stainless steel were determined from tensile tests.

Cylinder A was simultaneous pre-stressed by an internal pressure of 0.039×10^{6} N/m2 and an axial tensile force of 40 KN. Cylinder B had no pre-stressing.

Instrumentation consisted of load cells to measure the applied shear load together with displacement transducers to record the shear displacement of the top flance. A more detailed description of the shear buckling test rig used for cylinder A can be found in Reference 1.

3 BENCHMARK MODELS

The experimental models described in Section 2 were used as a basis for the benchmark calculation. With reference to Figure 1 the benchmark models can be described as:

Geometry	Cylinder A	Cylinder B
Radius (R)	0.253 m	0.100 m
Height (H)	0.253 m	0.100 m
Wall thickness (t)	0.914×10^{-3} m	1.2×10^{-3} m

Material Properties		
Modulus of Elasticity (E)	1.791×10^{11} N/m2	1.976×10^{11} N/m2
Poissons Ratio (ν)	0.26	0.3

Uni-Axial Stress-Strain Data

Cylinder A		Cylinder B	
σ (MN/m2)	ε %	σ (MN/m2)	ε %
125.4	0.07	213.5	0.00
174.0	0.10	278.0	0.05
217.0	0.14	296.0	0.10
239.0	0.19	306.0	0.15
261.0	0.40	311.6	0.20
283.0	0.87	314.0	0.25
304.0	1.67	316.0	0.30
326.0	2.61		

The cylinders were assumed to be clamped to the end flanges hence rotations at these edges were assumed to be zero. The lower flange during the experiments was assumed fully fixed to a rigid baseplate hence displacements here were also zero. The top flange is assumed to allow displacement in the vertical direction and in the direction of loading however due to its large stiffness the top flange is assumed to remain circular at all times.

Pre-stressing consisting of an internal pressure of 0.039 x 10^6 N/m2 and an axial tensile load of 40 KN was applied to cylinder A. Cylinder B had no pre-stressing. The shear load was applied to the top flange as a concentrated horizontal static force.

4 NUMERICAL METHODS

Two basic types of analysis were considered in the benchmark analysis i.e. eigenvalue and incremental non-linear. The eigenvalue buckling analysis can be further subdivided into linear elastic and non-linear bifurcation analysis.

4.1 Eigenvalue Analysis

For a linear elastic material, this is the usual Euler formulation of the bifurcation problem of the equilibrium. This analysis yields to a generalized eigenvalue problem:

$$(\underset{\sim}{K}o + \lambda \underset{\sim}{S})\underset{\sim}{\Phi} = 0$$

where $\underset{\sim}{K}o$ denotes the linear stiffness matrix, λ, $\underset{\sim}{\Phi}$ the eigenvalues and associated eigenmodes. The stability matrix, $\underset{\sim}{S}$, is, in the general case, the sum of the geometrical stiffness matrix and the load stiffness matrix.

The computer codes INCA and NOVNL have been further developed so that a first estimation of the buckling load sensitivity to plasticity, can be obtained by the solution of an initial bifurcation problem, in which plasticity is taken into account, within a finite theory, by the introduction of a material stiffness matrix into the matrix S of the Euler bifurcation problem (Reference 2).

Both the subspace method and the bloc-Lanczos method can be employed for the solution of the eigenvalue problem. Moreover, the problem can be better conditioned by eigenvalue shifting.

4.2 Incremental Complete Analysis

Both geometrical and material nonlinearities can be combined in the Newton-Raphson type iterative incremental analysis.

Increments are defined with respect to the loads, displacements or the automatic step-size method of Riks-Wempner.

For the incremental complete analysis, instability (bifurcation or limit point type of buckling) corresponds to the occurence of a negative pivot within the triangularisation of the tangent stiffness matrix. However, better agreement with experiment can possibly be obtained by investigating the occurence of plastic bifurcation before numerical instability is detected. For simplicity this can be done in the frame of the finite theory of plasticity. Plastic bifurcation is treated differently by the various codes. For example BILBO (CASTEM) solves the following eigenvalue problem:

$$(\underset{\sim}{K}p + w^2 \underset{\sim}{S})\underset{\sim}{\phi} = 0$$

where $\underset{\sim}{K}p$ is the tangent stiffness matrix computed using the tangent modulus formulation. Both $\underset{\sim}{K}p$ and $\underset{\sim}{S}$ are computed on the basis of the actual configuration for the current load level λ^*. If w^2 is equal to one λ^* is the nonlinear bifurcation load.

5 ANALYTICAL RESULTS AND COMPARISON WITH EXPERIMENT

The two benchmark cases detailed in Section 3 have been analysed by three different computer programs ABAQUS, CASTEM (INCA/BILBO) and NOVNL. The analytical and experimental results for each case are given in Tables I and II and illustrated graphically in Figures 2 and 3. These results are discussed in the following sections.

5.1 Elastic (Euler) Bifurcation Analysis

The calculated Euler load was found to be dependent on the mesh refinement of the finite element model used in the analysis. The finer the mesh the lower the calculated Euler buckling load. Taking into account the slight differences in mesh refinement it is seen that all of the codes predict buckling loads of the same order. A technique exists (Reference 1) whereby analytic bifurcation loads, obtained from 'coarse meshes' can be extrapolated to an asymptotic Euler buckling load which corresponds to an infinitely refined mesh. It was also discovered that the Donnel-Timoshenko formula (1) which predicts the buckling of a cylinder under pure torsion is apparently applicable to this specific problem.

$$\tau = \frac{E}{1-\nu^2}\left(\frac{t}{H}\right)^2\left[4.6 + \sqrt{7.8 + 1.76\left(\sqrt{1-\nu^2}\cdot\frac{H}{2Rt}\right)^{3/2}}\right] \qquad (1)$$

This formula gave buckling loads comparable to the values predicted by the finite element analyses.

It can be seen from the results that in each case the bifurcation analysis over-estimated the experimental bifurcation load. In the case of cylinder A the margin is around 50% (120 KN analytic - 77 KN experimental) whereas for cylinder B, when plasticity effects are significant the margin is over 400% (= 250 KN computed - 62 KN experimental).

5.2 Elastic-Plastic Bifurcation Analysis

When plasticity is accounted for in the eigenvalue problem the calculated bifurcation loads agree much more closely with the experimental values. The calculated elastic-plastic bifurcation loads were all less than 10% greater than the experimental value.

An empirical expression given by Galletly and Blachut (Reference 3) was found to give reasonable estimates of the experimental bifurcation load for these two problems.

$$\frac{1}{\tau_P^2} = \frac{1}{\tau_Y^2} + \frac{1}{\tau_E^2} \qquad (2)$$

where τ_P = Plastic shear stress at bifurcation load
τ_Y = Shear stress at yield point (0.2% strain for stainless steel)
τ_E = Critical shear stress for torsional buckling
$= 0.74E\,(R/H)^{0.5}(t/R)^{0.5}$

5.3 Non-Linear Incremental Analysis

Non-linear incremental analyses were carried out on both geometric perfect and imperfect models. Geometric imperfections were considered to be parallel to the first eigenmode and scaled to a maximum magnitude of between 10% and 66% of the wall thickness. These analyses indicated that buckling loads for both of these cylinders were insensitive to geometrical imperfection. This result has also been observed experimentally (Reference 3).

It was observed that the computed limit loads were over-estimated by a maximum of 25% in the case of cylinder A and 5% in the case of cylinder B.

It should be noted that no analysis accurately predicted the initial elastic regime in the experimental load-displacement relation. This is probably due to an accumulation of approximations made in the finite element model e.g. boundary conditions, material properties etc. This phenomenon is not untypical in buckling analyses.

A further point to note is that the buckled shape when non-linearities are considered is different from the Euler case in that the number of shear waves around the circumference is reduced. The non-linear incremental analysis correctly predicted the number of shear waves.

6 CONCLUSION

The benchmark problem of shear buckling of a thin cylinder was solved by three different computer codes and compared with experiment. These codes performed reasonably well and consistently with respect to each other in calculating the buckling response. It was observed that elastic (Euler) bifurcation analyses over-predicted the experimental bifurcation load by large margins. Elasto-plastic bifurcation analysis, where available gives good approximations to the experimental bifurcation loads. The complete non-linear incremental analyses calculated limit loads between 5%-25% greater than the experimental value.

Simplified expressions were found to predict bifurcation loads acceptably for these problems although further work is necessary to validate these expressions for geometries outside the limited range studied here.

ACKNOWLEDGEMENTS

The work was part of the Benchmark Calculations Programme of the Working Group on Codes and Standards Activity No. 2 and was part funded by the Commission of the European Communities, Brussels. The authors gratefully acknowledge the contribution of E.G. Carnoy formerly working with Novatome, France for solving the benchmark problem on the NOVNL code.

REFERENCES

Dostal, M. et al. Benchmark Study of Shear Buckling of a Cylindrical Vessel - CEC Nuclear Science and Technology Report EUR/6592 EN

Carnoy,E. Panosyan, G. 1984. Approximation of the Plastic Buckling Load as the Solution of an Eigenvalue Problem. Nuclear Eng. Design, Vol 78 347-354

Galletly, G.D. and Blachut, J. May 1985. Plastic Buckling of Short Vertical Cylindrical Shells subjected to Horizontal Edge Shear Loads. ASME Journal of Pressure Vessel Technology

TABLE I

SUMMARY OF ANALYTICAL RESULTS, CYLINDER A (Loads in KN)

Analysis Type	ABAQUS (RIKS)	ABAQUS	INCA/BILBO	NOVNL
Elastic Euler Buckling Load	125	135	130	120
Extrapolated Euler Buckling Load		100		
Axisymmetric Euler Buckling			110	
Timoshenko-Donnell Critical Load (equation 1)	101	101	101	101
Elasto-plastic initial bifurcation load	-	-	-	73
Experimental bifurcation load	-	-	-	-
Galletly-Blachut Critical load (equation 2)	65	65	65	65
Incremental Limit Load 0.4 mm Maximum Defect	86	97*	90**	104
Experimental Limit Load	77	77	77	77

* 0.1 mm maximum defect
** 0.0 mm maximum defect

TABLE II

SUMMARY OF ANALYTICAL RESULTS, CYLINDER B (Loads in KN)

Analysis Type	ABAQUS (RIKS)	ABAQUS	INCA/BILBO	NOVNL
Elastic Euler Buckling Load	306	334	250	289
Extrapolated Euler Buckling Load		268		
Axisymmetric Euler Buckling			290	
Timoshenko-Donnell Critical Load (equation 1)	298	298	298	298
Elasto-plastic initial bifurcation load	-	-	64	70
Experimental bifurcation load	61	61	61	61
Galletly-Blachut Critical load (equation 2)	65	65	65	65
Incremental Limit Load 0.12 mm Maximum Defect	86	86	-	82
Experimental Limit Load	78	78	78	78

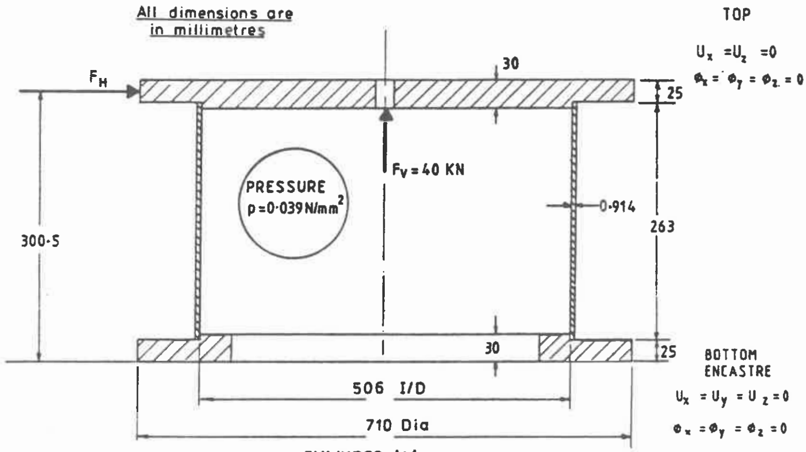

CYLINDER 'A'

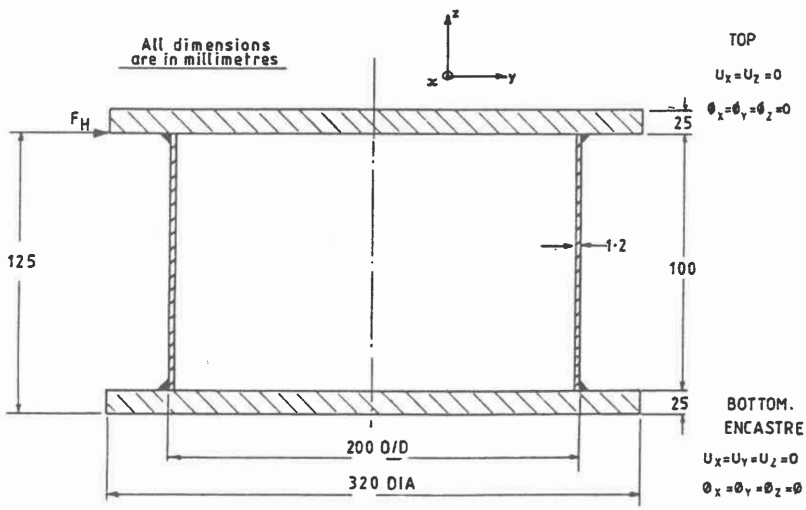

CYLINDER 'B'

FIGURE 1 BENCHMARK MODELS

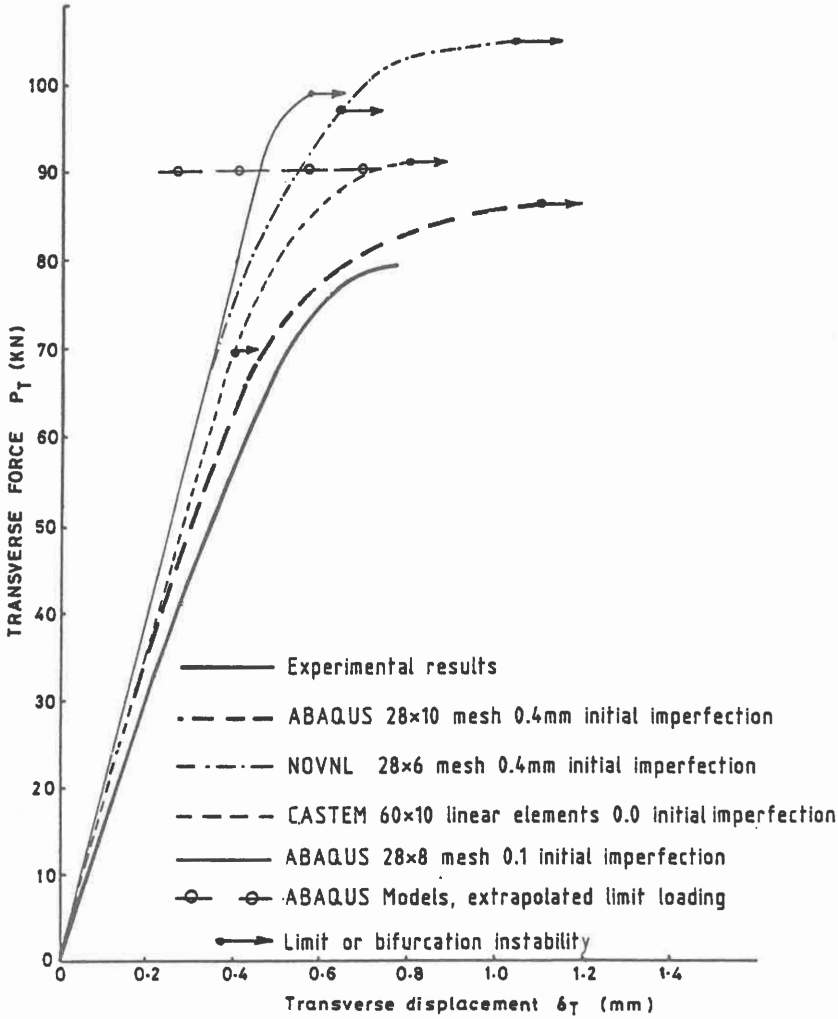

FIGURE 2 COMPARISON OF EXPERIMENTAL AND ANALYTICAL RESULTS, CYLINDER A

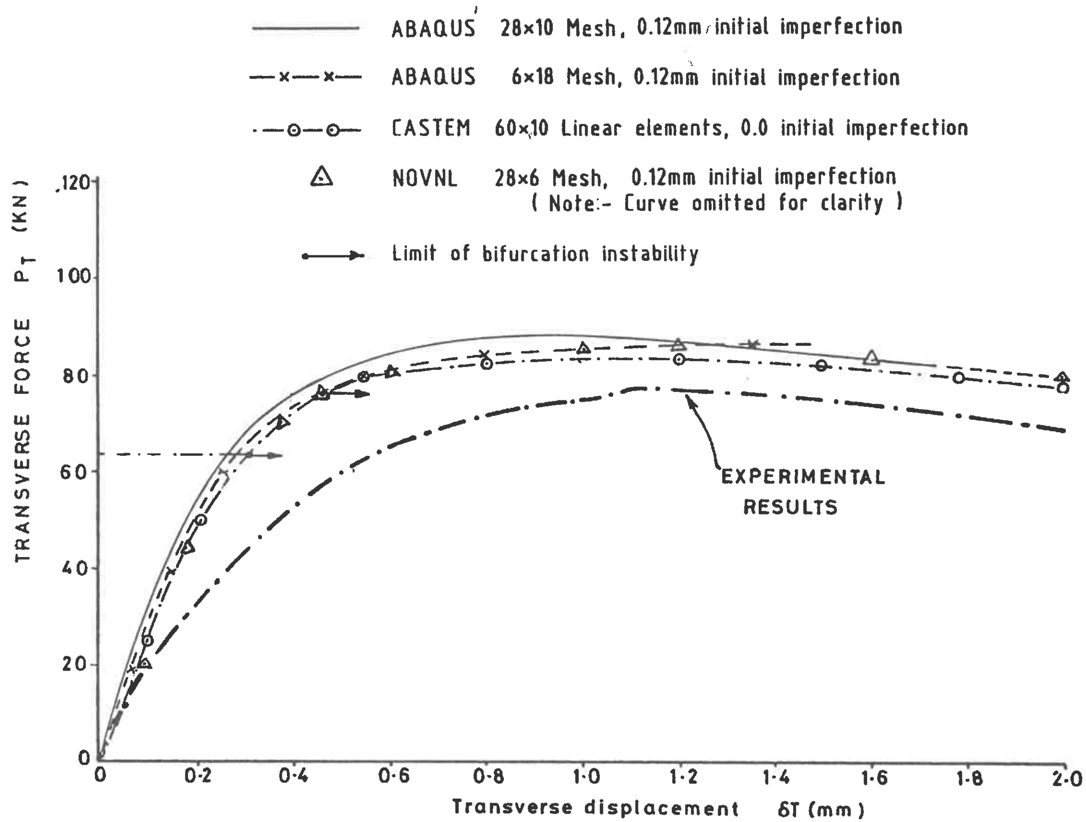

FIGURE 3 COMPARISON OF EXPERIMENTAL AND ANALYTICAL RESULTS, CYLINDER B